Electronic Supplementary Material (ESI) for CrystEngComm.

Supporting Information

The Lewis Acidic and Basic Character of the Internal HKUST-1 Surface Determined by Inverse Gas Chromatography

Alexander Münch and Florian Mertens

Table of Contents

1. Theoretical aspects of Inverse Chromatography

The relationship between the measured retention volume in gas chromatographic experiments and the thermodynamic adsorption parameters is given be the equation:

$$\ln V_N = \ln\left(RTn_s\right) + \frac{\Delta S_{ads}}{R} - \frac{\Delta H_{iso}}{R} \cdot \frac{1}{T} \tag{1}$$

The derivation of this equation is based on the assumption that all gaseous components of the mobile phase behave ideally. Thus, assuming equilibrium, the chemical potential of the analyte in the adsorbed state μ_s is equal to that of the analyte in the gas phase μ_g:

$$\mu_s = \mu_g = \mu^\circ(T) + RT\ln\frac{p_g}{p_0} \tag{2}$$

The difference between the chemical potential of the adsorbate and the chemical potential of the analyte in its standard state of pure vapor at 1 bar, μ°, is defined as the Gibbs free energy of adsorption ΔG_{ads} and is given by:

$$\Delta G_{ads} = \mu_s - \mu^\circ(T) = RT\ln\frac{p_g}{p_0} \tag{3}$$

ΔG_{ads} can also be determined by the equilibrium constant of adsorption K, called the partition coefficient, and is defined as the ratio of the amount of the adsorbate per volume on the substrate q_s and the amount of the adsorbate per volume in the gas phase c_{gas} at a given column temperature T:

$$K = \frac{q_s}{c_{gas}} \tag{4}$$

Using the ideal gas law $c_{gas} = n/v = p/RT$ and equation (4) the relationship (3) can be written as:

$$K = RTq_s\exp\left(-\frac{\Delta G_{ads}}{RT}\right) \tag{5}$$

The partition coefficient is also defined by the net retention volume V_N and the volume of the solid adsorbent V_S, $V_N/V_S = K$, and is called phase ratio. With K and the Gibbs-Helmholtz equation $\Delta G_{ads} = \Delta H_{ads} - T\cdot\Delta S_{ads}$, a functional relationship for the net retention volume V_N is then given by:

$$V_N = RTV_sq_s\exp\left(-\frac{\Delta G_{ads}}{RT}\right) = RTn_s\exp\left(\frac{\Delta S_{ads}}{R} - \frac{\Delta H_{iso}}{RT}\right) \tag{6}$$

or expressed linearly in 1/T by:

$$\ln V_N = \ln\left(RTn_s\right) + \frac{\Delta S_{ads}}{R} - \frac{\Delta H_{iso}}{R} \cdot \frac{1}{T} \qquad (7)$$

in which n_s is the total amount of the adsorbed analyte.

Although the determination of thermodynamic parameters from gas chromatographic experiments is usually not accepted for the provision of high precision data for thermodynamic databases where direct calorimetric measurements are the standard, inverse chromatography bears several advantages:[S1-S5]: (1) The temperature dependence of the evaluated surface parameters is inherently measured. (2) The limit of infinite dilution as a well-defined state of adsorption is almost generally fulfilled. (3) The sample purity requirements are not very strict because of the separation properties of the capillary. (6) The method of IGC is a very fast and can be conducted with standard equipment. In this paper, we will focus only on the determination of thermodynamic adsorption data.

****

Estimate of the nonspecific contribution to the Gibbs free energy of interaction(equation 6 in the main document)

In its fundamental work on molecular forces, London[S6,S7] connects the quantities dipole moment, polarizability, and ionization potential so that several versions of equations exist that describe the nonspecific part of the van der Waals interaction that are called London dispersion interaction. The mathematical derivation by Donnet[S8] et al. for experimetal determination of this interaction by the chromatographic means starts from the version of the London dispersion equation

$$-\Delta G_L = \frac{3}{2} \cdot h \cdot \frac{\nu_1 \nu_2}{\nu_1 + \nu_2} \cdot \alpha_{O,1} \cdot \alpha_{O,2} \cdot \frac{N_A}{4\pi\varepsilon_0{}^2} \cdot \left(\frac{1}{r_{1,2}}\right)^6 \qquad (7)$$

That containes beside the polarizability α_O of the two interacting molecules, here the substrate and the analyte, also their the characteristic electronic frequencies ν. The latter quantity is related to the first one by the expression:

$$\nu_i = \frac{1}{2\pi}\cdot\sqrt{\frac{e^2}{\alpha_{O,i}m_e}} \tag{8}$$

To simplify (7) which describes the interaction between molecule 1 and 2, the term $\frac{\nu_1\nu_2}{\nu_1+\nu_2}$ can be substituted by $\frac{\sqrt{\nu_1\nu_2}}{2}$ leading, given typical values, to an error of less than 4 %[S8]. Using this approximation and equation (7) the following function for the description of the potential energy between two nonidentical molecules can be obtained:

$$-\Delta G_{nonspec} = -\Delta G_L = \frac{3}{4}\cdot\frac{N_A}{4\pi\varepsilon_0^{2}}\cdot\left(\frac{1}{r_{1,2}}\right)^6\cdot\left(h\nu_1\right)^{1/2}\alpha_{O,1}\cdot\left(h\nu_2\right)^{1/2}\alpha_{O,2} \tag{9}$$

Since $-\Delta G_{interact} = RT\cdot\ln V_N + C = \left|-\Delta G_{spec}\right| + \left|-\Delta G_{nonspec}\right|$ holds, a functional relation for the determination of the free specific interaction energy can be derived using the equations (9) and (10):

$$\begin{aligned}\left[-\Delta G_{interact}\right] &= \left[-\Delta G_{nonspec}\right] + \left[-\Delta G_{spec}\right] = RT\ln V_N + C\\ &= \left[K\cdot\left(h\nu_S\right)^{\frac{1}{2}}\alpha_{O,S}\cdot\left(h\nu_L\right)^{\frac{1}{2}}\alpha_{O,L}\right] + \left[-\Delta G_{spec}\right]\end{aligned} \tag{10}$$

with $K = 3N_A/\left(\left(2\cdot 4\pi\varepsilon_0\right)^2\cdot r_{S,L}^6\right)$ where the subscripts S and L refer to the solid surface and the analyte. Thus with $\left(h\nu_L\right)^{\frac{1}{2}}\alpha_{O,L}$ being the specific property, $-\Delta G_{spec}$ can be determined by first determining the prefactor $K\cdot\left(h\nu_S\right)^{\frac{1}{2}}\alpha_{O,S}$, from the reference line of the *n*-alkanes by plotting $RT\ln V_N$ versus $\left(h\nu_L\right)^{\frac{1}{2}}\alpha_{O,L}$ and taking the value of the slope and then calculating the difference between $-\Delta G_{interact}$ and the value of the reference line at the value of the specific property of the analyte to be investigated. The slope of the linear function (10), $K\cdot\left(h\nu_S\right)^{\frac{1}{2}}\alpha_{O,S}$, is characteristic for a given solid surface and is related to the London dispersive interaction component of this surface[61]. The required electronic deformation polarizabilities can be taken from suitable references[S9], calculated either by using the Debye equation or the by the increment method according to Miller et al.[S10].

****

The relationship between thermodynamic data obtained by chromatograpich methods and by isochoric calorimetric experiments

The chromatographic determination o thermodynamic adsorption data yields the enthalpie of adsorption. Calorimetric, experiments, however,are often conducted at constant volume. Assuming the idla gas behavior the conversion is simple, but unfortunately there is a great deal of confusion present in the literature about these conversions, partly caused by the calamitous practice to write $q_{iso} = q_{diff} + RT_{av}$ as $|\Delta H_{iso}| = |\Delta H_{diff}| + RT_{av}$ instead of $|\Delta H_{iso}| = |\Delta U_{diff}| + RT_{av}$ and the convention to define heats of adsorption with the opposite sign compared to the general thermodynamic practice, which is to count the heat release from the system in question positively $\Delta H_{ads} = \Delta U_{ads} + p\Delta V_{ads} = \Delta U + p\Delta V_{ads}-V_{gas}) \approx \Delta U_{ads} - pV_{gas} = \Delta U_{ads} - RT$ with the sign convention for heats of adsorption $-q_{iso} = \Delta H_{ads} = \Delta U_{ads} - RT = -q_{diff} - RT$ results in $q_{iso} = q_{diff} + RT = |\Delta H_{ads}| = |\Delta U_{ads}| + RT$

2. HKUST-1 General Information and analysis of the synthesized HKUST-1 bulk material

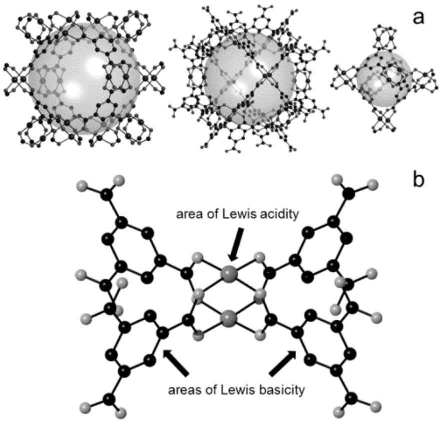

Figure S 1 a. Graphical illustration of the three different cavities of HKUST-1 with diameters of 12.1 Å, 10.3 Å, and 4.7 Å. b. Structural presentation of the typical binding pattern of the copper paddle wheel secondary building unit and the linker 1,3,5-benzenetricarboxylic acid of HKUST-1 showing the areas of Lewis acidity and basicity. Black, light gray, and gray spheres represent C, O, and Cu atoms, respectively. Hydrogen atoms have been omitted for clarity.

General characterization

Powder X-ray diffractograms were measured on a Phillips X´Pert diffractometer using a Cu Kα radiation (λ = 1.541 Å, 40 kV, 30 mA) source and a Bragg-Brentano setting. SEM images and EDX scans were taken using a Jeol JSM 7001F scanning electron microscope with an EDX-detector made by Bruker. The samples were coated by a thin gold layer to achieve electric conductivity.

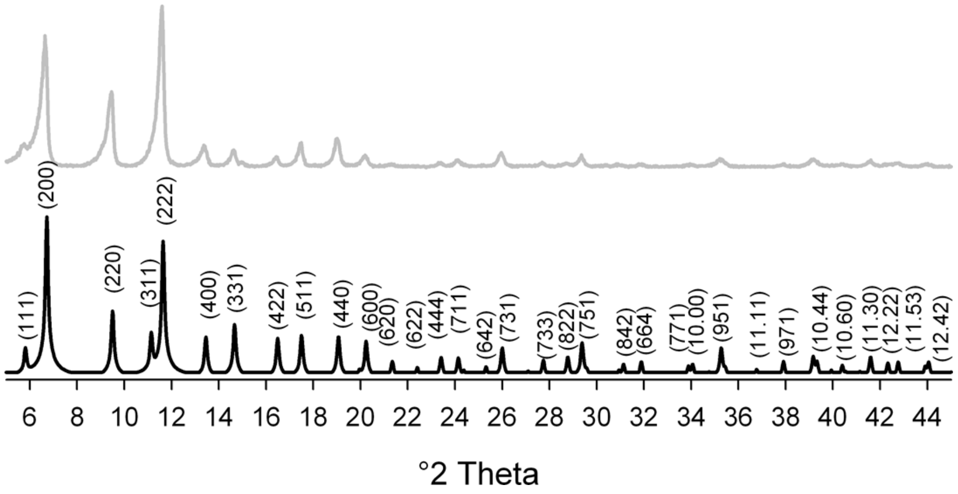

Figure S 2. Powder X-ray diffraction pattern of the synthesized HKUST-1 bulk material (gray) in comparison to the diffraction simulated from single crystal data (black). Only the most intensive reflexes are indexed.

The different ratios of the intensities of the measured reflections and the apparent missing of the (311) reflections (gray) in comparison to the single crystal data (black) can be explained by water adsorption from humid air during the measurement. This effect is described by Schlichte et.al.[S11]

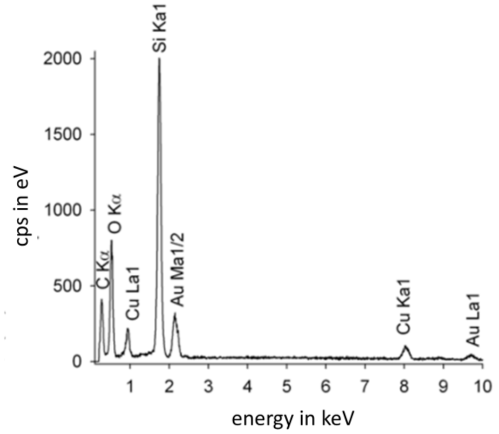

Figure S 3 EDX-spectrum of the MOF-coating on the wall inside the chromatographic column. The gold peaks belong to the conduction layer of the SEM-samples.

The energy-dispersive X-ray spectroscopic measurement of a typical area of the coating layer shows all elements except hydrogen, i.e. copper, carbon, and oxygen, which HKUST-1 is comprised of.

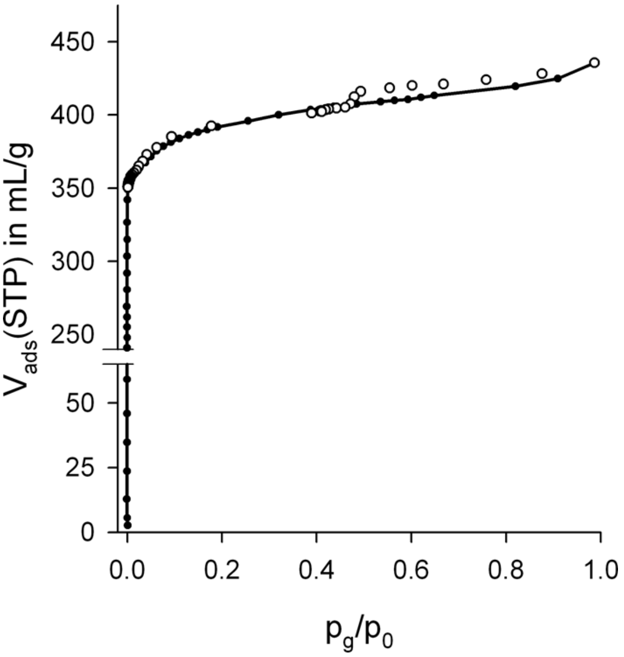

Figure S 4. Nitrogen adsorption isotherm of the synthesized HKUST-1 bulk material. ● – values of adsorption; ○ – values of desorption. A(BET) = 1168 m^2/g; A(BET-Snurr) = 1570 m^2/g.

The nitrogen (99.999 %, Praxair) adsorption isotherm was measured with a self-constructed Sievert apparatus under cryo-adsorption condition at 77K. The calibration was conducted with Helium (99.999 %, Praxair). The BET-surface area value A(BET) was calculated using the standard evaluation interval of 0.05 – 0.35 p/p_0. For the value of A(BET-Snurr) the modified evalution procedure according to Snurr et. al. for microporous materials was used.[S12]

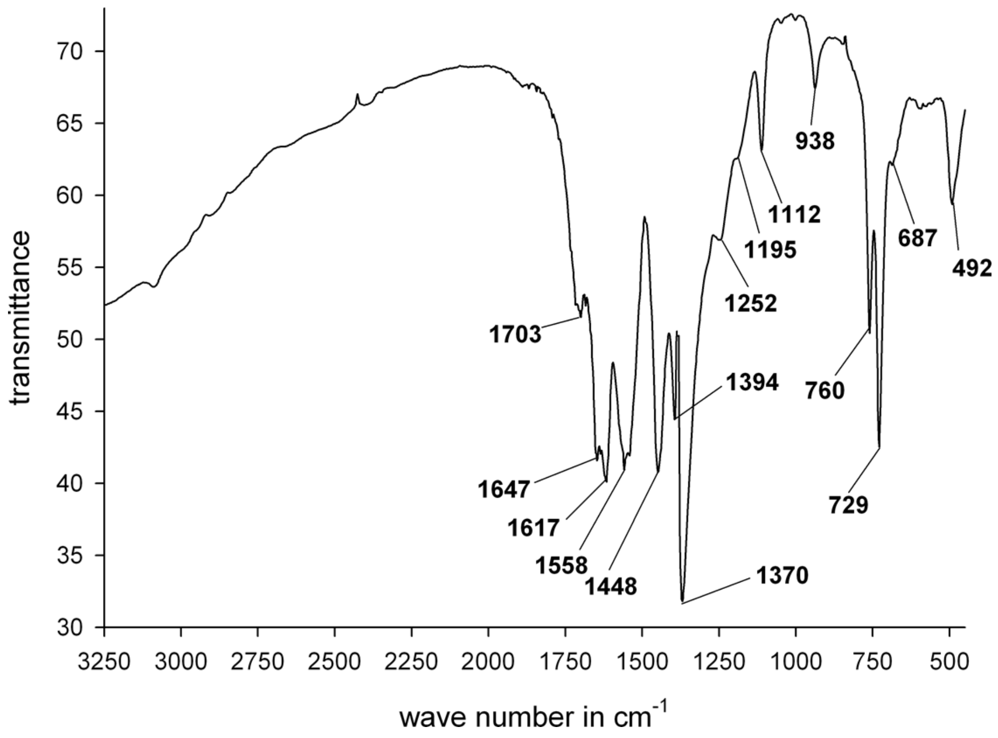

Figure S 5. Infrared spectrum of HKUST-1 measured in a KBr-pellet.

3. Physicochemical properties of the investigated analytes

Table S 1. Boiling points bp and polarizabilities α of the investigated analytes.

	bp in °C	α in cm^3

cyclohexan	80.7	$1.10\cdot10^{-23}$
benzene	80.1	$1.07\cdot10^{-23}$
n-pentane	36.1	$1.00\cdot10^{-23}$
n-hexane	68.7	$1.19\cdot10^{-23}$
n-heptane	98.4	$1.36\cdot10^{-23}$
diisopropyl ether	68.4	$1.25\cdot10^{-23}$
diethylether	34.5	$1.02\cdot10^{-23}$
tetrahydrofuran	65.0	$0.79\cdot10^{-23}$
di-*n*-propyl ether	90.1	$1.28\cdot10^{-23}$

4. XRD- and FTIR-data of HKUST-1 exposed to various analytes

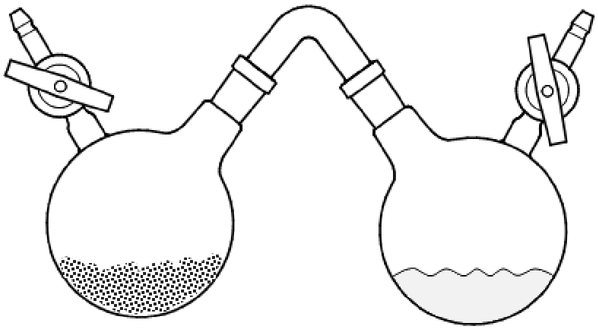

Figure S 6. Apparatus used for the adsorption of volatile compounds on HKUST-1 under inert conditions.

X-ray diffraction and Infrared Spectroscopic investigations of the analyte – HKUST-1 interaction

In order to provide further evidence that the specific interactions are mainly caused by the interaction between the analyte oxygen atoms and the HKUST-1 open metal sites, infrared spectroscopic measurements were conducted with the completely desolvated

MOF and samples each prepared by exposing desolvated HKUST-1 solely to one of the analytes. Prior to these measurements, the adsorbate-MOF systems were investigated by X-ray powder diffraction. The corresponding diffractograms, which are displayed in Figure S7, indicate that the crystalline network remains intact when exposed to the investigated analytes. The comparison of the diffractograms among each other and with the one simulated from single crystal data shows that the reflection intensities significantly differ and that the appearance of the diagrams essentially allows to devide them into two groups. One group of diagrams relates to the oxygen (ethers) and the other to the non-oxygen containing analytes. The diagrams of the ethers show an enhancement of the (222) reflection intensity which is not found in the case of benzene and cyclohexane. The same effect was observed in the case of the adsorption of water on the HKUST-1 SBU as described by Schlichte et al.[S1].

The corresponding IR spectra of these systems are displayed in Figure S8a und S8b. In comparison to cyclohexane, some IR-bands of benzene in the adsorbed state are shifted in comparison to those of the free molecule, which indicates that the benzene molecules more strongly interact than the completely hydrogenated counterpart. In addition, the bands, which are shifted, indicate a specific coordination mode. Because of the changes of the values of the stretching modes ν (CH) and the out-of-plane vibrational modes (o.o.p.) (CH), a π-π stacking interaction between the aromatic rings of the MOF-linker and the benzene rings can be postulated.

In the case of the adsorbed ethers on HKUST-1, the influence of the specific and nonspecific interactions of these molecules also leads to changes in the values of different vibrational bands. The specific adsorption phenomena are indicated by the symmetric and asymmetric stretching modes ν_s(C-O-C) and ν_{as}(C-O-C). Despite the very similar boiling points, diisopropyl ether displays a much shorter retention time than tetrahydrofuran. This fact can be explained by assuming a weaker interaction between the ether oxygen of diisopropyl and the open metal sites of the HKUST-1 SBU than in the case of THF. Some support for this view comes from the observation that the shifts to lower frequencies (wave numbers) of the ν_s(C-O-C) and ν_{as}(C-O-C) bands accompanying the adsorption processes on HKUST-1 are stronger in the case of tetrahydrofuran than in the case of diisopropyl ether (Figure S8b). Similar observations were made for the other two ethers. In summary, the spectroscopic data also support the presence the specific interaction between high electron density of the oxygen free electron pairs and the unsaturated coordination site of the copper(II)-ions of the MOF-SBU. In addition, the unaffected frequency values of the bands related to the alkyl parts of the ethers indicate their weak involvement in the energetics of the whole interaction process. The qualitative spectroscopic results are in accordance with the quantitative ones obtained by the inverse gas chromatographic analysis.

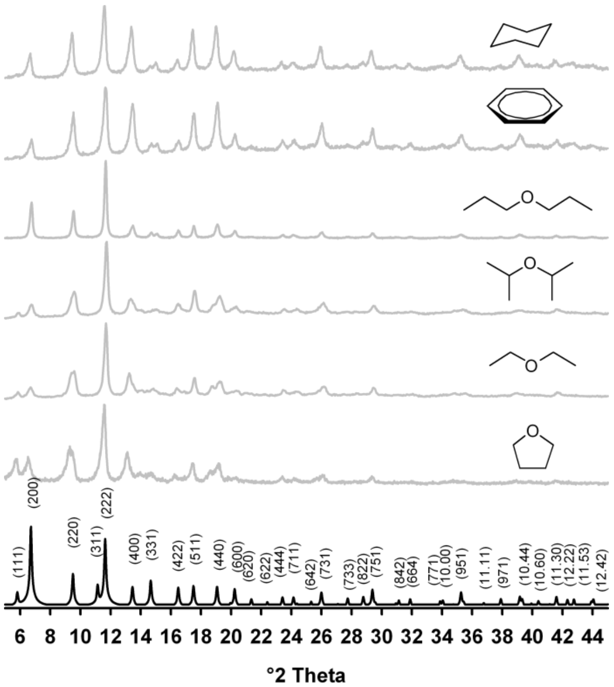

Figure S7 X-ray powder diffractions of the adsorbate complexes of the different analytes on HKUST-1 in comparison to the diffractogram simulated from the single crystal data. Only the most intensive reflections are indexed.

Infrared spectroscopic measurements

The IR-spectra of pure HKUST-1 and the analytes adsorbed on HKUST-1 in KBr-pellets were measured by a Varian 3100 FTIR (Fourier transform infrared) spectrometer. The pellets were prepared in an argon-filled Glovebox using KBr with a purity of 99.999 % (ABCR). For the pure HKUST-1 sample, the synthesized MOF was completely desolvated under vacuum at a temperature of 373 K for 2 hours. For the analyte – HKUST-1 adsorption experiments, each analyte was dried over sodium (99.8 %, ABCR) and adsorbed on pure HKUST-1 samples under inert conditions using Schlenk flasks and a distillation bridge.

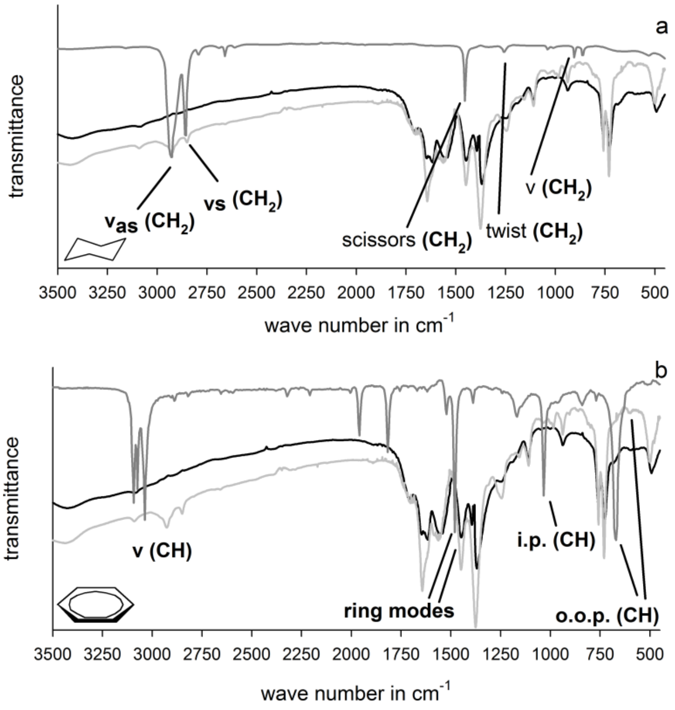

Figure S8a FTIR spectra of HKUST on with adsorbed benzene and cyclohexane

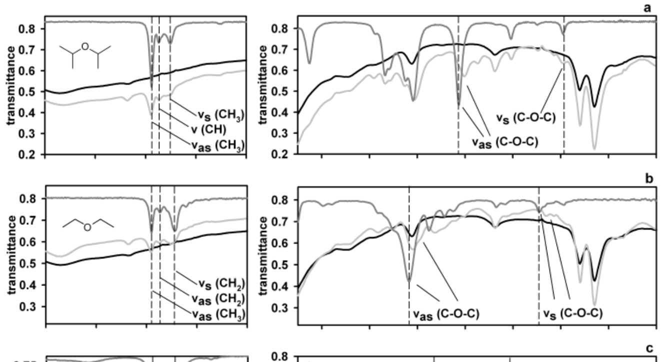

Figure S8b Infrared spectroscopic investigation of the adsorption of different analytes on HKUST-1 a – diisopropyl ether, b – diethyl ether, c – tetrahydrofuran, and d – di-*n*-propyl ether.

Table S 2. IR-data of cyclohexan.

	ν_{as} (CH_2)	ν_{as} (CH_2)	scissors (CH_2)	twist (CH_2)	ν (CH_2)
pure cyclohexane	2925 cm^{-1}	2860 cm^{-1}	1456 cm^{-1}	1260 cm^{-1}	905 cm^{-1}

adsorbed cyclohexane	2927 cm^{-1}	2850 cm^{-1}	covered	covered	904 cm^{-1}

The assignment is done via the comparison of the values of the measured bands and the values determined by Takahashi et.al.(S13)

Table S 3. IR-data of benzene.

	ν (CH)	ring modes	i.p. (CH)	o.o.p. (CH)
pure benzene	3121 cm^{-1} 3110 cm^{-1} 3092 cm^{-1} 3080 cm^{-1}	1480 cm^{-1}	1033 cm^{-1}	669 cm^{-1}
adsorbed benzene	3089 cm^{-1} 3034 cm^{-1} 2960 cm^{-1} 2928 cm^{-1}	covered	1037 cm^{-1}	598 cm^{-1}

The assignment is done via the comparison of the values of the measured bands and the values determined by Preuss et.al.(S14)

Table S 4. IR-data of diisopropyl ether.

	ν_{as} (CH_3)	ν (CH)	ν_s (CH_3)	ν_{as} (C-O-C)	ν_s (C-O-C)
pure diisopropyl ether	2969 cm^{-1}	2936 cm^{-1}	2871 cm^{-1}	1016 cm^{-1}	795 cm^{-1}
adsorbed diisopropyl ether	2972 cm^{-1}	2934 cm^{-1}	2875 cm^{-1}	1002 cm^{-1}	795 cm^{-1}

The assignment is done via the comparison of the values of the measured bands and the values determined by Beć et.al.(S15)

Table S 5. IR-data of diethyl ether.

	ν_{as} (CH_3)	ν_s (CH_2)	ν_{as} (CH_2)	ν_{as} (C-O-C)	ν_s (C-O-C)
pure diethyl ether	2977 cm^{-1}	2864 cm^{-1}	2933 cm^{-1}	1122 cm^{-1}	845 cm^{-1}
adsorbed diethyl ether	2977 cm^{-1}	2877 cm^{-1}	2937 cm^{-1}	1098 cm^{-1}	831 cm^{-1}

The assignment is done via the comparison of the values of the measured bands and the values determined by Wieser et.al.(S16)

Table S 6. IR- data of tetrahydrofuran.

	ν_{as} (CH_2-O)	ν_s (CH_2-O)	ν_{as} (C-O-C)	ν_s (C-O-C)
pure tetrahydrofuran	2941 cm^{-1}	2875 cm^{-1}	1070 cm^{-1}	919 cm^{-1}

adsorbed tetrahydrofuran	2976 cm^{-1}	2876 cm^{-1}	1043 cm^{-1}	890 cm^{-1}

The assignment is done via the comparison of the values of the measured bands and the values determined by Gadioli et.al.(S17)

Table S 7. IR-data of di-*n*-propyl ether

	ν_{as} (CH$_3$)	ν_{as} (CH$_2$)	ν_s (CH$_3$)	ν_s (CH$_2$)	ν_{as} (C-O-C)	ν_s (C-O-C)
pure di-*n*-propyl ether	2963 cm^{-1}	2937 cm^{-1}	2877 cm^{-1}	2857 cm^{-1}	1122 cm^{-1}	953 cm^{-1}
adsorbed di-*n*-propyl ether	2963 cm^{-1}	2932 cm^{-1}	2875 cm^{-1}	2958 cm^{-1}	1070 cm^{-1}	937 cm^{-1}

The assignment is done via the comparison of the values of the measured bands and the values determined by Muszyński et.al.(S18)

5. Capillary coating

The chromatographic capillaries were coated according to the protocol described in the main document using a simple self-built coating apparatus depicted below.

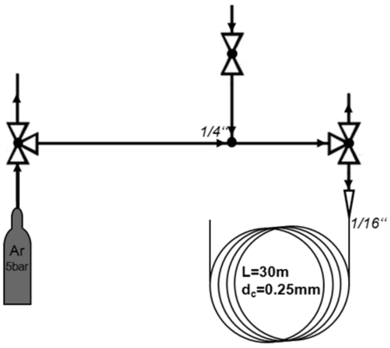

Figure S9 Self-constructed apparatus for the deposition of HKUST-1 in chromatographic capillaries via a cyclic layer preparation technique.

6. Results of the chromatographic separations

Table S 8. Adjusted retention time t_r’ of cyclohexane and benzene at 443.15 K, 453.15 K, 463.15 K, and 473.15 K.

	t_r’ in min at 443.15 K	t_r’ in min at 453.15 K	t_r’ in min at 463.15 K	t_r’ in min at 473.15 K
cyclohexane	1.5248 ± 0.0072	1.1390 ± 0.0120	0.8656 ± 0.0090	0.6730 ± 0.0053
benzene	2.1290 ± 0.0147	1.5498 ± 0.0283	1.1476 ± 0.0160	0.8780 ± 0.0118

Table S 9. Retenion volume V_N of cyclohexane and benzene at 443.15 K, 453.15 K, 463.15 K, and 473.15 K.

	V_N in ml at 443.15 K	V_N in ml at 453.15 K	V_N in ml at 463.15 K	V_N in ml at 473.15 K
cyclohexane	3.5945 ± 0.0170	2.6926 ± 0.0284	2.0591 ± 0.0215	1.5956 ± 0.0127
benzene	5.0188 ± 0.0348	3.6637 ± 0.0670	2.7299 ± 0.0381	2.0817 ± 0.0280

Table S 10. Adjusted retention time t_r’ of diisopropyl ether, diethyl ether, tetrahydrofuran, and di-*n*-propyl ether at 493.15 K, 503.15 K, 513.15 K, and 523.15 K.

	t_r’ in min at 493.15 K	t_r’ in min at 503.15 K	t_r’ in min at 513.15 K	t_r’ in min at 523.15 K
diisopropyl ether	2.9045 ± 0.1972	2.0610 ± 0.0102	1.4380 ± 0.0468	0.9915 ± 0.0235
diethyl ether	4.5033 ± 0.4547	2.3113 ± 0.0903	2.3113 ± 0.0903	1.5735 ± 0.0386
tetrahydrofuran	17.1958 ± 2.3352	12.7705 ± 0.0599	8.7270 ± 0.3608	5.8210 ± 0.1620
di-*n*-propyl ether	27.0310 ± 3.1981	19.4695 ± 0.1468	12.7465 ± 0.3813	8.2218 ± 0.1700

Table S 11. Retention volume V_N of diisopropyl ether, diethyl ether, tetrahydrofuran, and di-*n*-propyl ether at 493.15 K, 503.15 K, 513.15 K, and 523.15 K.

	V_N in ml at 493.15 K	V_N in ml at 503.15 K	V_N in ml at 513.15 K	V_N in ml at 523.15 K
diisopropyl ether	6.0026 ± 0.4075	4.3502 ± 0.0216	2.9810 ± 0.0970	2.0530 ± 0.0487
diethyl ether	9.3067 ± 0.9397	7.0071 ± 0.0220	4.7912 ± 0.1871	3.2581 ± 0.0800
tetrahydrofuran	35.5377 ± 4.8260	26.9550 ± 0.1264	18.0911 ± 0.7480	12.0528 ± 0.3354
di-*n*-propyl ether	55.8639 ± 6.6091	41.0947 ± 6.6094	26.4235 ± 0.7905	17.0238 ± 0.3520

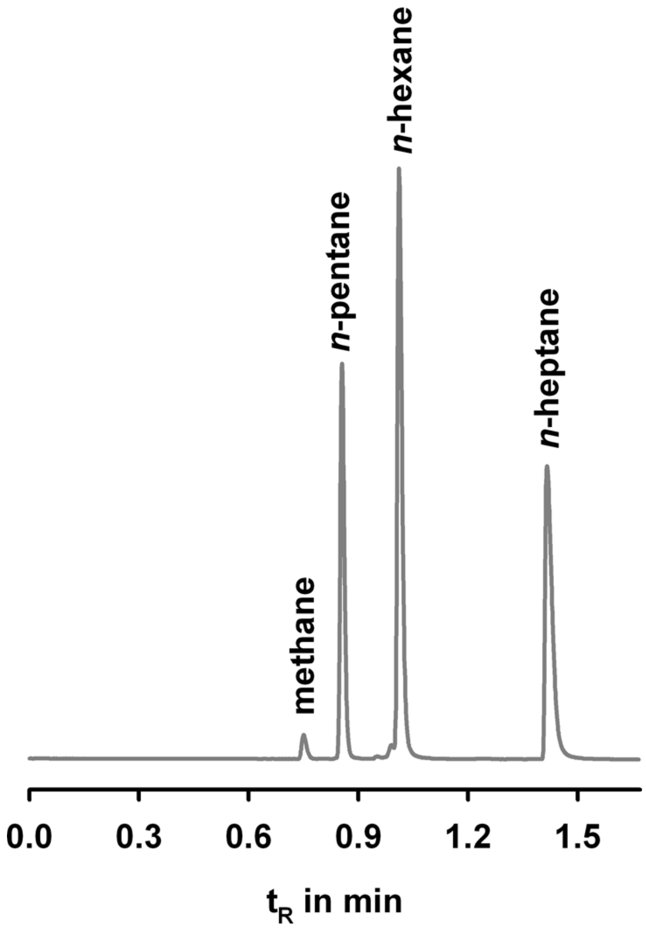

Figure S 10. Chromatographic separation of n-pentane, n-hexane, and n-heptane at a temperature of 523.15 K and a gas flow of 4.15 mL/min by an HKUST-1 coated capillary.

Table S 12. Adjusted retention time t_r' of *n*-pentane, *n*-hexane, and *n*-heptane at 493.15 K, 503.15 K, 513.15 K, and 523.15 K.

	t_r' in min at 493.15 K	t_r' in min at 503.15 K	t_r' in min at 513.15 K	t_r' in min at 523.15 K
n-pentane	0.2026 ± 0.0011	0.1646 ± 0.0018	0.1360 ± 0.0091	0.1050 ± 0.0012
n-hexane	0.5552 ± 0.0037	0.4358 ± 0.0043	0.3446 ± 0.0109	0.2644 ± 0.0042
n-heptane	1.5644 ± 0.0079	1.1846 ± 0.0105	0.9002 ± 0.0203	0.6760 ± 0.0124

Table S 13. Retention volume V_N of *n*-pentane, *n*-hexane, and *n*-heptane at 493.15 K, 503.15 K, 513.15 K, and 523.15 K.

	V_N in ml at 493.15 K	V_N in ml at 503.15 K	V_N in ml at 513.15 K	V_N in ml at 523.15 K
n-pentane	0.4171 ± 0.0023	0.3383 ± 0.0037	0.2802 ± 0.0188	0.2174 ± 0.0025
n-hexane	1.1430 ± 0.0076	0.8958 ± 0.0088	0.7099 ± 0.0225	0.5265 ± 0.0084
n-heptane	3.2206 ± 0.0163	2.4350 ± 0.0217	1.8544 ± 0.0418	1.3997 ± 0.0258

7. Thermodynamic data from the chromatographic separation of *n*-pentane, *n*-hexane, and *n*-heptane

Table S 14. Values of adsorption enthalpies, entropies, and adsorption Gibbs free energies of, *n*-pentane, *n*-henxane, and *n*-heptane (T_{av} = 508.15 K).

	n-pentane	*n*-hexane	*n*-heptane
$-\Delta H_{diff}$ in $kJ\cdot mol^{-1}$	46.0	54.8	59.5
$-\Delta H_{iso}$ in $kJ\cdot mol^{-1}$	50.2	58.0	63.7
$-\Delta S_{ads}$ in $J\cdot K^{-1}\cdot mol^{-1}$	100.4	110.0	110.8
$-\Delta G_{ads}$ in $kJ\cdot mol^{-1}$	-0.8	3.2	7.4

The chromatographic separation experiments were performed using a mixture of *n*-pentane (Riedel-de Haën, 99.8 %), *n*-hexane (VWR, 98%), and *n*-heptane (Merck, > 99 %) at the ratios 1 : 1 : 1. The chromatograms for the determination of the adsorption enthalpies and entropies of the alkanes were recorded with the pure substances at a constant inlet carrier gas flows of 4.15 mL/min and at different temperature which were varied from 493.15 K to 523.15 K. During the gas chromatographic measurements, the ambient temperature was 25 °C and the corresponding pressure was 0.969 bar. The dead time was determined by the retention time of methane.

8. Nonspecific interaction linear reference functions obtained from the adsorption data of pentane, hexane, and heptane for the determination of the specific adsorption Gibbs free energies

493.15 K: $-\Delta G_{interact} = 3.96\cdot 10^{52}\ V^{0,5}\cdot J\cdot C^{1/3}\cdot m^{-2}\cdot mol^{-1}\cdot (h\nu)^{0,5}\alpha_{O,L} - 35737.10\ J\cdot mol^{-1}$,

$R^2 = 0.9974$.

503.15 K: $-\Delta G_{interact} = 3.90\cdot 10^{52}\ V^{0,5}\cdot J\cdot C^{-1,5}\cdot m^{-2}\cdot mol^{-1}\cdot (h\nu)^{0,5}\alpha_{O,L} - 36207.75\ J\cdot mol^{-1}$;

$R^2 = 0.9974$.

513.15 K: $-\Delta G_{interact} = 3.81\cdot 10^{52}\ V^{0,5}\cdot J\cdot C^{-1,5}\cdot m^{-2}\cdot mol^{-1}\cdot (h\nu)^{0,5}\alpha_{O,L} - 36395.36\ J\cdot mol^{-1}$;

$R^2 = 0.9973$.

523.15 K: $-\Delta G_{interact} = 3.82\cdot 10^{52}\ V^{0,5}\cdot J\cdot C^{-1,5}\cdot m^{-2}\cdot mol^{-1}\cdot (h\nu)^{0,5}\alpha_{O,L} - 37727.61\ J\cdot mol^{-1}$;

$R^2 = 0.9949$.

9. Experimental data for benzene (t'_r, V_N, $\Delta G_{interact}$, ΔG_{spec}, and $\Delta G_{nonspec}$)

t_r’ in min at 493.15 K	0.6073 ± 0.0098
t_r’ in min at 503.15 K	0.4970 ± 0.0028
t_r’ in min at 513.15 K	0.3878 ± 0.0070
t_r’ in min at 523.15 K	0.2993 ± 0.0085
V_N in ml at 493.15 K	1.2439 ± 0.0197
V_N in ml at 503.15 K	1.0182 ± 0.0058
V_N in ml at 513.15 K	0.7948 ± 0.0144
V_N in ml at 523.15 K	0.6170 ± 0.0174
$-\Delta G_{interact}$ in $kJ\cdot mol^{-1}$ at 493.15 K	0.9
$-\Delta G_{interact}$ in $kJ\cdot mol^{-1}$ at 503.15 K	0.01
$-\Delta G_{interact}$ in $kJ\cdot mol^{-1}$ at 513.15 K	-1.0
$-\Delta G_{interact}$ in $kJ\cdot mol^{-1}$ at 523.15 K	-2.1
$-\Delta G_{spec}$ in $kJ\cdot mol^{-1}$ at 493.15 K	2.8
$-\Delta G_{spec}$ in $kJ\cdot mol^{-1}$ at 503.15 K	3.0
$-\Delta G_{spec}$ in $kJ\cdot mol^{-1}$ at 513.15 K	2.8
$-\Delta G_{spec}$ in $kJ\cdot mol^{-1}$ at 523.15 K	3.0
$-\Delta G_{nonspec}$ in $kJ\cdot mol^{-1}$ at 493.15 K	-1.9
$-\Delta G_{nonspec}$ in $kJ\cdot mol^{-1}$ at 503.15 K	-2.9
$-\Delta G_{nonspec}$ in $kJ\cdot mol^{-1}$ at 513.15 K	-3.8
$-\Delta G_{nonspec}$ in $kJ\cdot mol^{-1}$ at 523.15 K	-5.1

!!! Please note that the the specific interaction Gibbs free enthaply of benzene is essentially temperature independent.

10. Determination of ΔH_{spec} and ΔS_{spec} from temperature dependent measurements

diisopropyl ether: $-\Delta G_{spec} = 21106.4\ J\cdot mol^{-1} - 32.1\ J\cdot K^{-1}\cdot mol^{-1} \cdot T$; $R^2 = 0.9705$.

diethyl ether: $-\Delta G_{spec} = 30627.7\ J\cdot mol^{-1} - 37.0\ J\cdot K^{-1}\cdot mol^{-1} \cdot T$; $R^2 = 0.7167$.

tetrahydrofuran: $-\Delta G_{spec} = 39717.8\ J\cdot mol^{-1} - 32.6\ J\cdot K^{-1}\cdot mol^{-1} \cdot T$; $R^2 = 0.8701$.

di-*n*-propyl ether: $-\Delta G_{spec} = 28654.8\ J\cdot mol^{-1} - 30.1\ J\cdot K^{-1}\cdot mol^{-1} \cdot T$; $R^2 = 0.8701$.

benzene: $-\Delta G_{spec} = 1043.3\ J\cdot mol^{-1} + 3.6\ J\cdot K^{-1}\cdot mol^{-1} \cdot T$; $R^2 = 0.3421$.

Table S 15. Values of the specific adsorption enthalpies and entropies of benzene and the investigated ether molecules.

	$-\Delta H_{spec}$ in $kJ\cdot mol^{-1}$	$-\Delta S_{spec}$ in $J\cdot K^{-1}\cdot mol^{-1}$
diisopropyl ether	21.1	-32.1
diethyl ether	30.6	-37.0
tetrahydrofuran	39.7	-32.6
di-*n*-propyl ether	28.6	-30.1
benzene	1.0	3.6

Please not that the values for the specific interaction of benzene are small. This is in accordance with the fact that, given the temperature independence of $-\Delta G_{spec}$, the entropy contribution should vanish.

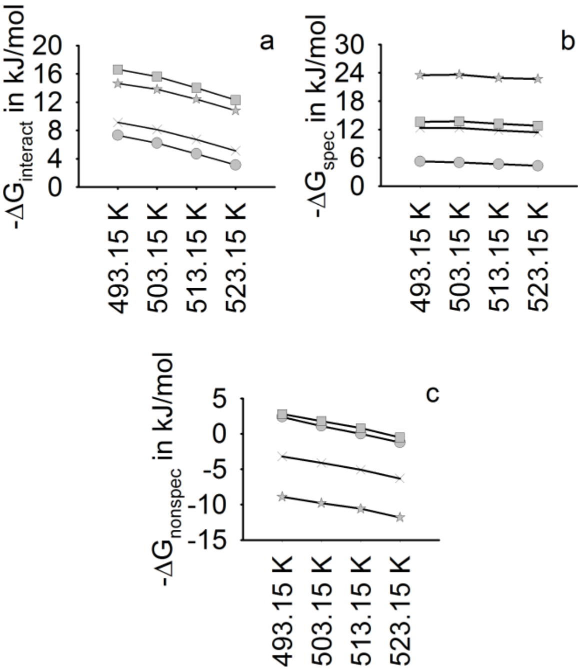

Figure S 11 Interaction Gibbs free energy (a), specific interaction Gibbs free energy (b), and nonspecific interaction Gibbs free energy (c) as functions of the temperature. ● – diisopropyl ether. × – diethyl ether. * – tetrahydrofuran. ■ – di-*n*-propyl ether.

11. Thermogravimetric investigation of the ether-HKUST-1 complexes

The thermogravimetric investigation of the ether-HKUST-1 complexes was carried out with a Setaram Sensys TGA-DSC by ramping the temperature from 25 °C to 450 °C with a rate of 5 $K \cdot min^{-1}$.The samples were kept all the time under argon atmosphere..

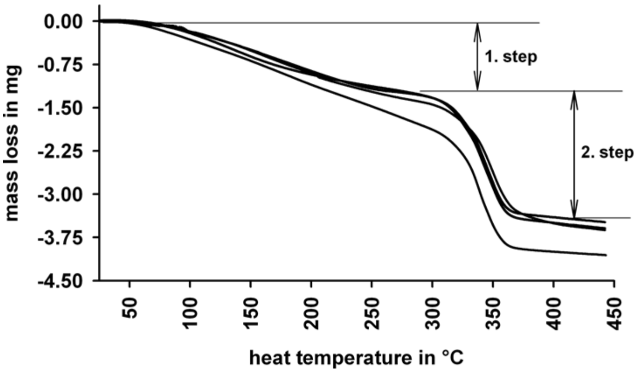

Figure S 12. Thermogravimetric investigation of the ether-HKUST-1 complexes. Step one reflects the desorption of the ethers from the MOF-lattice and step two the decomposition of HKUST-1. Diisopropyl ether: Δm = -19.4 % is consistent with composition of HKUST-1 $Cu_3(BTC)_2{\cdot}(H_2O)_3$ plus 1.41 molecules of diisopropyl ether. Diethyl ether: Δm = -17.5 % is consistent with a composition of HKUST-1 plus 1.75 molecules of diethyl ether. Tetrahydrofuran: Δm = -21.9 % is consistent with a composition of HKUST-1 plus 2.37 molecules of tetrahydrofuran. Di-*n*-propyl ether: Δm = -23.9 % is consistent with a composition of HKUST-1 plus 1.98 molecules of di-*n*-propyl ether.

12. Schematic representation of the interactions of the investigated analytes with the HKUST-1 lattice

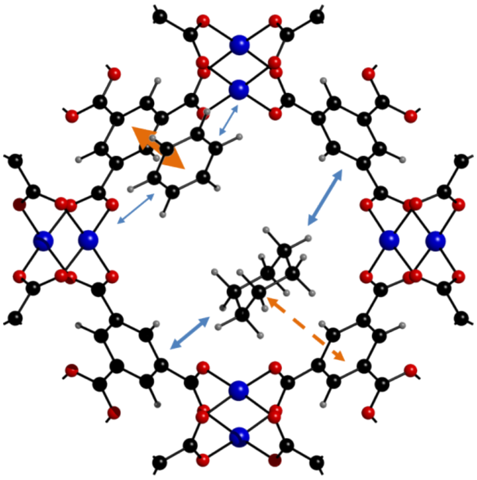

Figure S 13. Schematic representation of the adsorption of benzene and cylcohexane on HKUST-1.

a

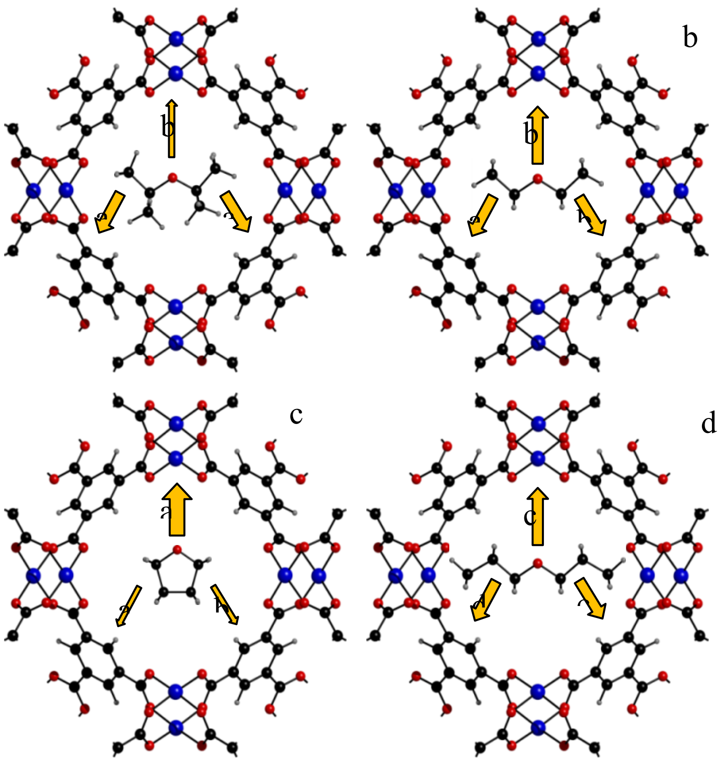

Figure S 14. Schematic representation of the adsorption of diisopropyl ether (a), diethylether (b), tetrahydrofuran (c), and di-*n*-propyl ether on HKUST-1.

13. Parameter Definitions

Greek letters

α_O	deformation polarizability
$\alpha_{O,L}$	deformation polarizability of the analyte
$\alpha_{O,S}$	deformation polarizability of the solid phase
γ_l^d	London component of the surface Gibbs free energy of the liquid analyte phase
ν	characteristic electronic frequency

Latin letters

a_{CH_2}	cross-sectional area of a methylene group
A_N	acceptor number of Gutmann
c_{gas}	amount of the adsorbate per volume of gas
C_A, C_B	empirical parameter represents the covalent interaction
D_N	donor number of Gutmann
E_A, E_B	empirical parameter represents the electrostatic interaction
F_a	volumetric flow-rate measures at ambient temperature
ΔG_{ads}	Gibbs free energy of adsorption
ΔG_{CH_2}	incremental Gibbs free energy of adsorption attributed to a methylene group
$\Delta G_{interact}$	interaction Gibbs free energy of adsorption
ΔG_L	dispersive Gibbs free energy of adsorption
ΔG_{spec}	specific interaction Gibbs free energy of adsorption
$\Delta G_{nonspec}$	nonspecific interaction Gibbs free energy of adsorption
ΔH_{iso}	isosteric enthalpy of adsorption

ΔH_{spec}	specific enthalpy of adsorption
j	James-Martin gas compressibility correction factor
K	partition coefficient
K_A	constant, which describe the Lewis acidity of the solid surface
K_B	constant, which describe the Lewis basicity of the solid surface
n	amount of substance
n_s	total amount of adsorbate in the adsorbate state (mol)
p	pressure
p_g	partial pressure
p_i	pressure of gas applied to the chromatogram
p_0	pressure of gas at outlet
q_s	amount of the adsorbate per volume of the adsorbent
q_{diff}	differential heat of adsorption
q_{iso}	isosteric heat of adsorption
$r_{1,2}$	distance between two molecules
ΔS_{ads}	entropy of adsorption
ΔS_{spec}	specific entropy of adsorption
T	column temperature
T_a	ambient temperature
T_{av}	average temperature for the interval studied
t_m	dead time
t_r	retention time
t_r'	adjusted retention time
ΔU_{diff}	differential energy of adsorption
V	volume
V_N	net retention volume
$V_{N,n}$	net retention volume of a *n*-alkane with n carbon atoms
$V_{N,n+1}$	net retention volume of a *n*-alkane with n+1 carbon atoms
V_S	volume of the solid adsorbent

Fundamental physical constant

ε_0	vacuum permittivity ($8.854 \cdot 10^{-12}$ F·m^{-1})
e	elementary charge ($1.602 \cdot 10^{-19}$ C)
h	Planck constant ($6.626 \cdot 10^{-34}$ J·s)
m_e	mass of electron ($9.109 \cdot 10^{-31}$ kg)
N_A	Avogadro constant ($6.022 \cdot 10^{23}$ mol^{-1})
R	ideal gas constant (8.314 J·K^{-1}·mol^{-1})

14. References

(S1) A. Voelkel and T. Grześkowiak, *J. Mater. Chem.*, 2001, **11**, 1289.

(S2) A. Voelkel, A. Krysztafkiewicz and T. Grześkowiak, *Adsorpt. Sci. Technol.*, 1999, **17**, 173.

(S3) A. Voelkel and T. Grześkowiak, *Chromatographia*, 2000, **51**, 608.

(S4) W. Wasiak, I. Rykowska and A. Voelkel, *J. Chromatogr., A*, 2002, **969**, 133.

(S5) A. Voelkel, *Chemom. Intell. Lab. Syst.*, 2004, **72**, 205.

(S6) F. London *Trans. Faraday Soc.*, 1937, **33**, 8b-26.

(S7) F. London, *Z. Physik*, 1930, **63**, 245.

(S8) J. B. Donnet, S. J. Park and H. Balard, *Chromatographia*, 1991, **31**, 434.

(S9) T. M. Miller, in *CRC Handbook of Chemistry and Physics*, ed. W. M. Haynes CRC Press, Boca Raton, 93rd ed., 2012, Ch. 10, pp. 187-196.

(S10) K. J. Miller and J. A. Savchik, *J. Am. Chem. Soc.*, 1979, **101**, 7206.

(S11) Schlichte, K.; Kratzke, T.; Kaskel, S. Improved synthesis, thermal stability and catalytic properties of the metal-organic framework compound $Cu_3(BTC)_2$. *Micropor. Mesopor. Mater.* **2004**, *73*, 81-88.

(S12) Bae, Y.-S.; Yazaydin, A. O.; Snurr, R. Q. Evaluation of the BET Method for Determining Surface Areas of MOFs and Zeolites that Contain Ultra-Micropores. *Langmuir* **2010**, *26*, 5475-5483.

(S13) Takahashi, H.; Shimanouchi, T.; Fukushima, K.; Miyazawa, T. Infrared spectrum and normal vibrations of cyclohexane. *J. Mol. Spectrosc.* **1964**, *13*, 43-56.

(S14) Preuss, M.; Bechstedt, F. Vibrational spectra of ammonia, benzene, and benzene adsorbed on Si (001) by first principles calculations with periodic boundary conditions. *Phys. Rev.* **2006**, *B73*, 155413-1 – 155413-8.

(S15) Beć, K. B.; Muszyński, A. S.; Michniewicz, N.; Wreszcz, W.; Kotynia, A.; Hawranek, J. P. Vibrational spectra of liquid di-*iso*-propylether. Vib. *Spetrosc.* **2011**, *55*, 44.

(S16) Wieser, H.; Laidlaw, W. G.; Krueger, P. J.; Fuhrer, H. Vibrational spectra and a valence force field for conformers of diethyl ether and deuterated analogues. *Spectrochim. Acta*, **1968**, *24A*, 1055.

(S17) Gadioli, B.; Gallinella, E.; Coulombeau, C.; Jobic, H.; Berthier, G. Geometric Structure and Vibrational Spectrum of Tetrahydrofuran. *J. Phys. Chem.* **1993**, *97*, 7844.

(S18) Muszyński, A. S.; Beć, K. B.; Wrzeszcz, W.; Michniewicz, N.; Mojak, A.; Hawranek, J. P. Vibrational spectra of liquid di-*n*-propylether. *J. Mol. Struct.* **2010**, *975*, 205.

Table of content (TOC) image